PCCP

Role of conductive binder to direct solid-electrolyte interphase formation over silicon anodes

Journal:	*Physical Chemistry Chemical Physics*
Manuscript ID	CP-ART-05-2019-002610.R1
Article Type:	Paper
Date Submitted by the Author:	20-Jun-2019

Complete List of Authors:	Browning, Katie; Oak Ridge National Laboratory, ; University of Tennessee Knoxville, Materials Science and Engineering Browning, Jim; Oak Ridge National Laboratory, Chemical and Engineering Materials Doucet, Mathieu; Oak Ridge National Laboratory, Yamada, Norifumi; High Energy Accelerator Research Organization Liu, Gao ; E O Lawrence Berkeley National Laboratory Veith, Gabriel; Oak Ridge National Laboratory, Materials Science and Technology Division

Role of conductive binder to direct solid-electrolyte interphase formation over silicon anodes

Katie L. Browning[a,b], James F. Browning[c], Mathieu Doucet[c], Norifumi L. Yamada[d], Gao Liu[e], and Gabriel M. Veith[b]

[a]Department of Materials Science and Engineering, University of Tennessee, Knoxville, TN 37996, United States
[b]Chemical Sciences Division and [c]Neutron Scattering Division, Oak Ridge National Laboratory, Oak Ridge, Tennessee 37831, United States
[d]Neutron Science Laboratory, High Energy Accelerator Research Organization, 203-1 Shirakata, Tokai, Naka, Ibaraki, 319-1106, Japan
[e]Electrochemistry Division, Lawrence Berkeley National Laboratory, San Francisco, California, United States

Abstract

With the use of *in situ* neutron reflectometry (NR) we show how the addition of an electronically conductive polymeric binder, PEFM, mediates the solid-electrolyte interphase (SEI) formation and composition on an amorphous Si (a-Si) electrode as a function of the state-of-charge. Upon initial contact with the electrolyte a Li rich, 41 Å thick, layer forms on the surface of the anode *below* the polymer layer. At 0.8 V (vs. Li/Li^+), a distinct SEI layer forms from the incorporation of electrolyte decomposition products in the reaction layer that is organic in nature. In addition, solvent uptake in the PEFM layer occurs resulting in the layer swelling to ~200 Å. Upon further polarization to 0.4 and 0.15 V (vs. Li/Li^+) a thick layer (800 Å) on the surface of the Si is evident where a diffuse interface between the PEFM and SEI occurs resulting in a matrix between the two layers, as the binder has taken up a large amount of electrolyte. The two layers appear to be interchanging solvent molecules from the PEFM to the SEI to the Si surface preventing the lithiation of the a-Si. By 0.05 V (vs. Li/Li^+) a Li rich, 72 Å thick, SEI layer condenses on the surface of the anode, and a 121 Å intermixed layer on top of the SEI with LiF and Li-C-O species is present with the rest blended in to the electrolyte.

Introduction

When fabricating composite battery electrodes, a slurry is prepared by dispersing the active material (electrode of study), conductive additive (typically a form of C), and a polymeric binder, used for mechanical strength and adhesion, in a solvent. After thorough mixing the slurry is cast onto a metal foil which acts as the current collector. The binder enhances the adhesion to the

current collector in addition to providing mechanical integrity among the blend of different materials. The choice of binder is particularly important for silicon anodes due to the extreme expansion, around 300%, during lithiation of the Si, where mechanical integrity is needed to prevent electronic isolation and pulverization of Si nanoparticles.(1,2) There is no standardized amount of binder added to the system but on average accounts for ~15 wt% of the total slurry.(3)

The most commonly used binder in the battery industry has been polyvinylidene fluoride (PVDF); however, Si based anodes with PVDF as the binder result in poor cycling performance.(3–5) This has led to an intensive research effort exploring different binders for use in Si anodes. The most commonly used binders to date have been polyacrylic acid (PAA) and Li substituted polyacrylic acid (LiPAA).(3,6) Their success as binders is attributed to the carboxylic groups that interact and bind with the -OH groups found on the native oxide layer on Si.(3) There has also been interest in electronically conductive binders in order to eliminate the need for conductive additives such as carbon black. One such example is PEFM, which was designed to incorporate different functional groups to create a n-type conductive polymer modified to uptake electrolyte and maintain mechanical stability.(7)

As a result of the volume changes in Si anodes, the Si surface cracks leading to exposure of fresh active surfaces causing further electrolyte degradation and the formation of additional SEI products leading to poor performance. Based on surface area and the large weight percent of added binder the surface of the Si should be fully coated, assuming a uniform dispersion, leading to the question of how this coating affects SEI formation? Does this SEI differ from that found on just Si? Furthermore, how does the ion transport or reduction processes occur within and/or through the insulating polymer layer? Only a few studies have focused on the complexity of binder interaction and their influence on SEI formation. For instance, in a photoelectron spectroscopy study looking at graphite-based anodes with water processable binders, the authors determined binder functional groups positively influence SEI formation.(8) Nguyen et al. compared SEI composition and formation on Si as a function of binder (PVDF, PAA, CMC, and a cross-linked PAA-CMC) using XPS.(9) The PVDF resulted in a thick SEI dominated by carbonate moieties in comparison with the PAA which accelerated the $LiPF_6$ decomposition leading to LiF and $Li_xPF_yO_z$, and a thin SEI that suppressed the reduction of the solvent decomposition.(9) This highlights the complex interactions among active material, binder, and conductive additive that are, in part, due to a large number of interfaces within cast electrodes.

The goal of this study is to explore some of these fundamental questions of the polymer/SEI interactions. To this end we use neutron reflectometry which allows the SEI growth and composition to be observed *in situ*. The technique utilizes thin films allowing for a controlled architecture and interface of a conductive binder and an amorphous Si (a-Si) thin film electrode. The chemical composition of the SEI can be further probed and characterized with x-ray photoelectron spectroscopy (XPS); however, due to the need to wash samples before using the technique some of the organic species are washed away or chemically altered. As a result, the combination of NR with XPS provides an extremely valuable tool to study and measure the SEI layer both *in situ* and *ex situ*.

Neutron reflectometry (NR) is ideally suited to study buried interfaces *in situ*. Neutrons can be reflected or refracted from interfaces between materials. Specular reflectivity is the probability of a neutron being reflected off of a surface as a function of the wave vector transfer Q perpendicular to the sample surface:

$$Q = \frac{4\pi sin\theta}{\lambda} \quad [1]$$

where θ is the angle of the incident beam and λ is the wavelength of the neutron. Modeling of the measured reflectivity yields information about the scattering length density (SLD, β) profile as a function of depth. The SLD is indicative of the material composition of the layer and can be expressed as:

$$\beta = \frac{\rho N_A}{M} \sum_i^n b_i \quad [2]$$

in which ρ is the material density, N_A Avogadro's number, M molecular weight, and b_i the coherent scattering length of the i^{th} atom within the material.

This technique has been utilized to study the SEI formation on amorphous Si anodes (a-Si).(10–13) These studies showed in direct contact with $LiPF_6$ electrolyte, a Li rich reaction layer forms atop the Si surface.(10) Studies using reflectometry have determined a "breathing" like behavior of the SEI where upon lithiation the layer thins and thickens upon de-lithiation.(11,12) Interestingly in another NR experiment looking at the SEI formation on Si with the addition of the additive fluoroethylene carbonate (FEC), the opposite effect was observed in which the SEI thickens during lithiation and thins during de-lithiation.(13)

In this study, the effect of the polymeric binder, Poly(2,7-9,9-dioctylfluorene-co-2,7-9,9-(di(oxy-2,5,8-trioxadecane))fluorene-co-2,7-fluorenone-co-2,5-1-methylbenzoate ester) (PEFM),

on the SEI layer composition was studied using *in situ* neutron reflectometry. The functional groups of the polymer include polyfluorene (P), fluorene (E), fluorenone (F), and a methyl benzoate ester (M).(7) PEFM was chosen as it was designed to incorporate components of what is believed to make a good binder, i.e., swelling when in contact with the electrolyte, mechanical integrity, and electronic conductivity to reduce the need for a conductive additive such as C.(7) In this work cells were cycled to various potentials associated with electrolyte reduction and lithiation of the silicon and NR data was collected. *Ex situ* experiments using x-ray photoelectron spectroscopy (XPS) were performed to further characterize species of the SEI at various formation potentials.

Experimental

Sample electrodes for this experiment were prepared by a combination of physical vapor deposition and spin coating. A single crystal 51 mm diameter, 5 mm thick silicon wafer was used as a substrate. The films were deposited using an in-house sputtering system utilizing RF magnetron sputtering and reaching base pressures in the 10^{-6} Torr range. A 6 nm Cu layer was deposited using a commercially available Cu target (99.99%, Plasmaterials). The Cu layer is used as a current collector, a contrast layer, and in addition, prevents lithiation of the single crystal Si substrate. Without breaking vacuum, a 50 nm a-Si (99.999%, Kurt J. Lesker) film was deposited atop the Cu film as the working electrode. The PEFM polymer binder was dissolved in chloroform to make a 0.1 wt% solution which was then pipetted onto the a-Si layer and then spun at 5000 rpm for 30 seconds. Samples were dried under vacuum at 80℃ for two hours to remove excess solvent and were subsequently vacuum sealed in order to prevent further air exposure.

The battery electrolyte was prepared using deuterated ethylene carbonate (d-EC, Sigma Aldrich, 99%) and deuterated dimethyl carbonate (d-DMC, Sigma Aldrich, 99%) in a 30:70 wt% and dried over zeolites in an Ar filled glovebox. A thin strip of Li was placed in the solvents in order to react away impurities. The $LiPF_6$ salt (BASF, 99.99% battery grade) was added to form a ~1.1 M solution.

An *in situ* electrochemical half-cell was constructed using the Cu/a-Si thin film. A TiZr ($Ti_{0.47}Zr_{0.53}$) substrate was used for the Li counter/reference electrode as it does not react with Li metal in addition to being a null neutron scatterer. A Teflon coated Viton o-ring, with a 1 mm cross-sectional area and 49 mm inner diameter, was placed between the a-Si and lithium coated

TiZr to prevent shorting and define the working area of the electrode. A Teflon top was placed between the TiZr and cell top to prevent shorting and 4 mL of electrolyte were introduced into the cell. A conductive Ag epoxy (ITW Electronics) was used for an electrical contact and did not come into contact with the electrolyte. The scattering orientation and photo of the electrochemical cell is shown in Figure S1. Cells were cycled at a C/3 rate and charged to the following potentials: 1.5, 1.2, 0.8, 0.4, 0.15, and 0.05 V (vs. Li/Li^+) using a Biologic VSP potentiostat. Once the potential was reached under galvanostatic conditions the current response was measured under potentiostatic conditions. After reaching the desired potentials the cell was allowed to equilibrate for ten minutes and NR data was collected. Before acquiring *in situ* measurements, samples were measured in air in order to determine the SLD profiles of the deposited layers.

Experiments were performed on the Soft Interface Analyzer (SOFIA) instrument (Beamline 16) at the Materials and Life Science Experimental Facility (MLF) located at the Japan Proton Accelerator Research Complex (J-PARC) in Tokai, Japan.(14,15) SOFIA is a horizontal geometry instrument that utilizes the time-of-flight method. The incident neutron energy ranges from $0.11 < \lambda < 0.88$ nm with a theta range of 0.3, 0.7, 1.6, 3.5° for in-air samples and 0.3, 0.7, 1.4, 2.4° for samples collected in the *in situ* cell. Data fitting was performed using the Motofit software developed by A. Nelson.(16)

Ex situ experiments using x-ray photoelectron spectroscopy (XPS) were performed using a PHI 3056 spectrometer with a Mg anode operated at a 15 kV with an applied power of 350 W. A low-resolution survey scan was collected with a pass energy of 93.5 eV, while high resolution scans utilized a pass energy of 23.6 eV. Spectra were corrected to 284.8 eV, the primary C peak for all samples as evidence of charging was present in the lithiated samples. Witness samples were prepared in the same manner as the NR sample; however, films were deposited onto Cu foil as opposed to a Si substrate. After spin coating the electrodes were cycled in a coin cell using the same electrochemical procedure as the NR experiment looking at OCV, 1.2 V, 0.8 V, 0.15 V, and 0.05 V. After reaching the desired potential the cells were disassembled and soaked in DMC to remove excess salt deposits and were then transported in a vacuum sealed container to the XPS.

Results

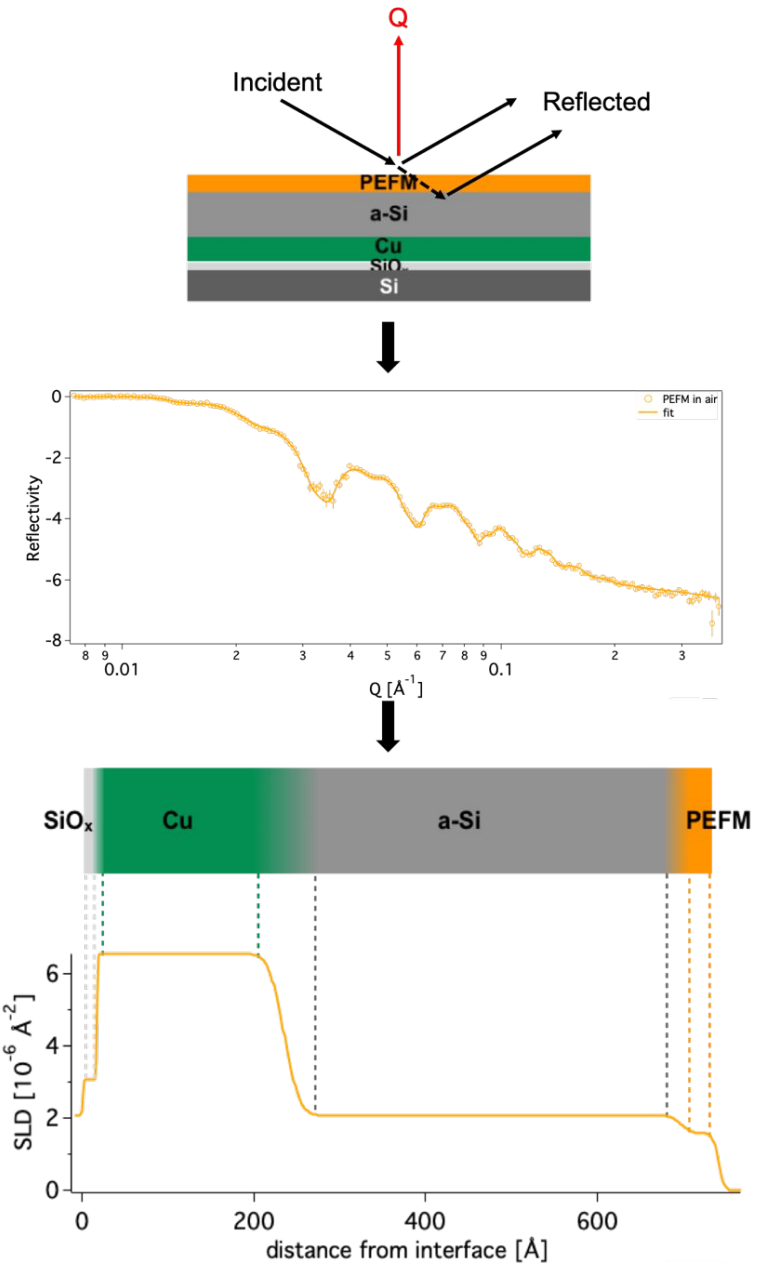

Figure 1. A representation of how data is collected on the thin film assembly (top) for the in-air measurements to determine the as-prepared sample structure. Data collections (middle) result in a reflectivity (R) vs. Q plot (open circles) and the resulting fit (solid line). The fit produces an SLD distribution (bottom) representing the structure of the film as a function of depth.

As-prepared Si anode. The a-Si anode used in the NR studies was initially measured in air to determine the as-prepared structure of the sample and is shown in the top of Figure 1. The refinement of the data (Figure 1 middle) results in a SLD distribution (Fig.1 bottom) which represents the structure of the film as a function of depth, as schematically shown on the SLD plot on the bottom of Figure 1. From the refinement, the Si layer was determined to have a thickness of ~464 Å with an SLD of 2.07 $x10^{-6}$ $Å^2$ (for simplicity the unit for the SLD [$x10^{-6}$ $Å^{-2}$] will be omitted from this point on), which is in agreement with the theoretical SLD of Si (2.07) indicating a uniform and dense a-Si film. There was no evidence of an oxide layer on the a-Si surface, which doesn't preclude the existence of one as such a thin layer is often hidden by roughness between adjacent layers or an SLD close to that of the a-Si or PEFM films.(13) The Cu film was approximately 200 Å thick with an SLD of 6.54 which is also in good agreement to that of the theoretical value of 6.59, while the native oxide layer present on the substrate was ~17 Å thick. The PEFM polymer binder was spin coated to a thickness of 41.9 Å, which was ideal in order to allow lithiation and prevent creation of an insulating layer. The fit resulted in an SLD of 1.56. With Equation 2 and the measured SLD value the density and areal density for the PEFM binder layer were calculated to be 0.35 g cm^{-3} and 0.15 μg cm^{-2}, respectively. Witness samples fabricated for XPS show the C1s peak with a significant amount of C-C/C-H (284.8 eV) on the surface most likely originating from the binder which has a complex structure made up of C ring backbones (Figure 3).(7) Approximately 25.4 at% of the C1s spectra (Figure S6) was made up of a C-O species with concurrent peaks observed in the O1s spectra (532.5 eV, Figure 4). There was additional evidence of carbonyl groups with a binding energy of 531.26 eV. The Si2p peak (Figure S2) is still evident which is expected as the binder layer is only a few nanometers thick while the depth probed by XPS is on the order of 10 nm.

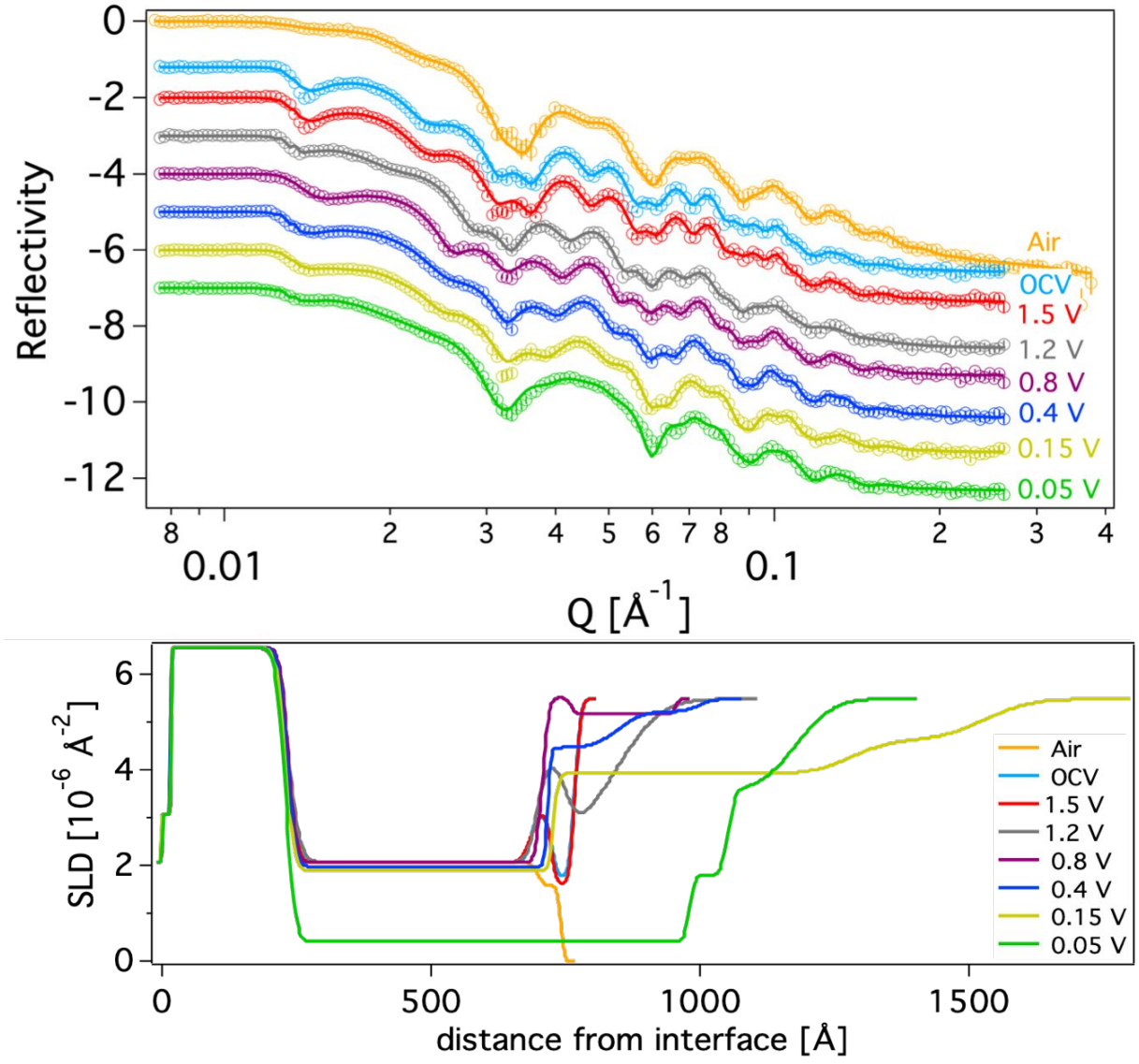

Figure 2. Neutron reflectivity data with open holes representing collected data and the fit shown as a solid line (top). The reflectivity has been offset for clarity. The SLD profile from resulting fit.

Open circuit voltage. After the cell was constructed and alignment complete the electrolyte was in contact with the anode for ~ 30 min and the OCV equilibrated to 2.8 V (vs Li/Li$^+$) before data collection. Figure 2 shows NR data collected for the sample in the cell (top) and resulting SLD vs thickness profiles (bottom) used to fit the data. Individual SLD depth profiles for each state of charge can be found in the supplemental section (Figure S7). Results for the thickness, SLD, and goodness of fit (χ^2) for the PEFM, SEI, and a-Si films are summarized in Table 1. Changes in the reflectivity from air to OCV are evident, with the resulting fit indicating a decrease in the Si layer

thickness (464.2 to 450.1 Å) and the addition of a new layer on the surface of the anode. The new film is attributed to a reaction layer that forms as a result of the chemical reactivity of the active Si surface with the electrolyte and is approximately 42 Å thick.(10) The SLD value was 2.95 significantly lower than the electrolyte SLD (5.46) indicating the incorporation of a component with a low coherent scattering length needed to lower the SLD. Given the elemental makeup of the electrolyte components, i.e. D, O, F, and P (6.6, 5.8, 5.1, and 5.6 fm, respectively), have relatively high scattering lengths, the reaction layer is most likely Li rich, which has a bound coherent scattering length of -1.90 fm, and would originate from the $LiPF_6$ salt.(10) The fitting routine of the neutron data attempted various models in terms of the placement of the reaction layer/SEI. When the layer was placed on the surface of the PEFM binder, the model resulted in a none physical representation of the system and could only be fitted with the layer underneath the binder. In addition, the only way to get a higher SLD is with the d-EC/d-DMC; therefore, the change has to be due to solvent at the a-Si interface. Turning to the XPS results the C1s spectra shows no statistical variation in C-C/C-H and C-O peaks between the in air and OCV witness samples (Figure 3). However, the O1s spectra shows the formation of C-O-C, P-O-F peak, as shown in Figure 4, attributed to the $LiPF_6$ salt in the electrolyte. There was a decrease of ~16 at% in the C=O while the C-O, Si-O peak stayed the same, in agreement with the C1s data (Figure S6). Interestingly the PEFM layer stays fairly constant in thickness (Table 1) with a very slight increase in SLD from 1.56 to 1.73. This increase would indicate an incorporation of 0.05 volume fraction of electrolyte incursion within the PEFM film from porosity or absorption. The F1s peak shows evidence of P-F (688.6 eV, 39.8 at%) and P-O-F (686.4 eV, 60.2 at%) representative of the salt (Figure 5) and further supported by the P2p peak with the addition of P-O (134.4 eV, Figure S3).

Table 1. Results for NR refinements of the PEFM, SEI, and a-Si layers.

Potential	PEFM Thickness (Å)	SLD (10^{-6} Å^{-2})	Roughness (Å)	SEI Thickness (Å)	SLD (10^{-6} Å^{-2})	Roughness (Å)	a-Si Thickness (Å)	SLD (10^{-6} Å^{-2})	Roughness (Å)	χ^2
Air	41.88±1	1.56±0.05	6.54±0.01				464.18±1	2.07±0.003	8.97±0.9	1.9
OCV	42.53±2	1.73±0.07	8.19±0.6	41.93±2	2.95±0.05	7.79±1	450.14±1	2.06±0.01	7.56±1	6.2
1.5 V	44.90±0.7	1.59±0.05	8.18±0.5	38.65±0.1	3.11±0.05	8.09±0.1	450.86±0.9	2.06±0.01	13.36±1	6.7
1.2 V	93.11±2	2.58±0.07	63.71±2	55.23±2	4.08±0.06	16.96±5.3e-14	461.82±0.7	2.06±0.01	13.65±0.9	5.6
0.8 V	199.41±0.6	5.21±0.03	6.72±0.8	54.82±2	5.52±0.04	7.66±1	472.51±0.4	2.06±0.01	7.66±1	2.9

0.4 V	147.17±2	5.19±0.04	19.75±1	130.39±3.5	4.47±0.03	37.39±1	484.52±0.4	1.92±0.03	6.46±0.30	2.8
0.15 V	247.07±4	4.62±0.05	68.60±1	556.13±4	3.91±0.03	5.14±0.14	499.84±0.5	1.89±0.03	5.14±0.14	3.4
0.05 V	121.28±1	3.09±0.05	91.34±1	71.62±1	1.63±0.06	6.40±0.9	747.92±2	0.433±0.03	6.54±2.05e-14	7.7

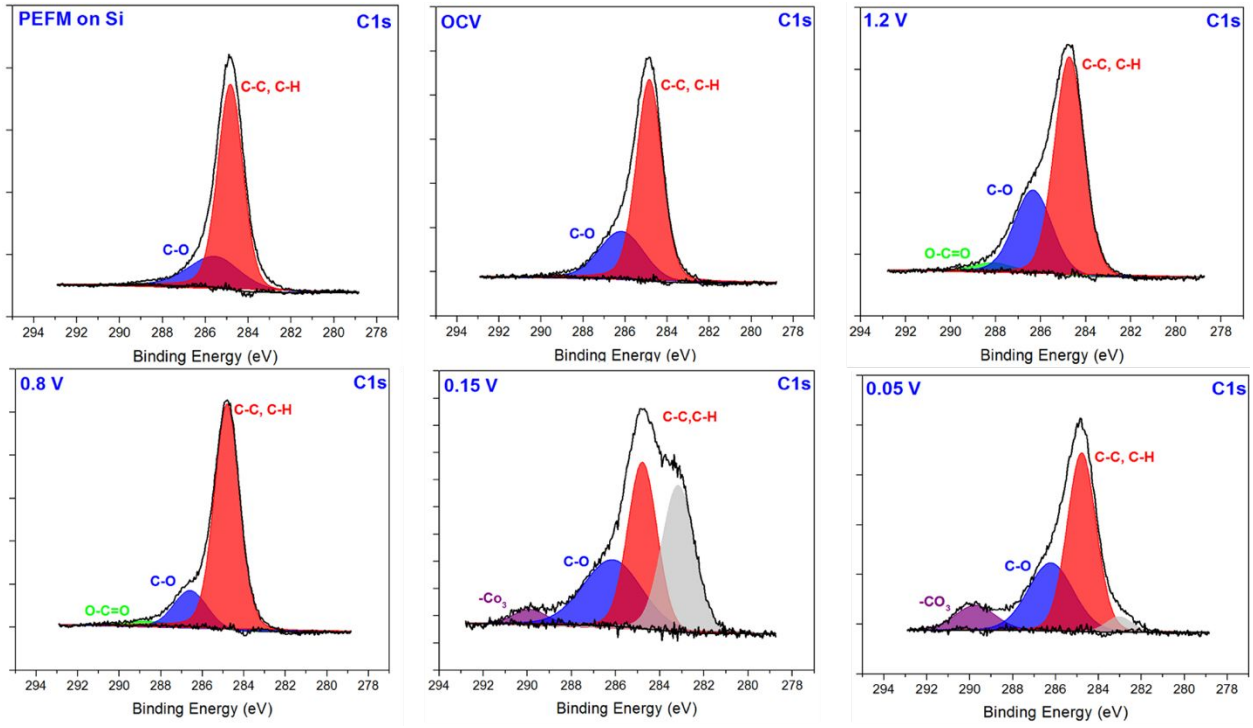

Figure 3. XPS results for C1s spectra

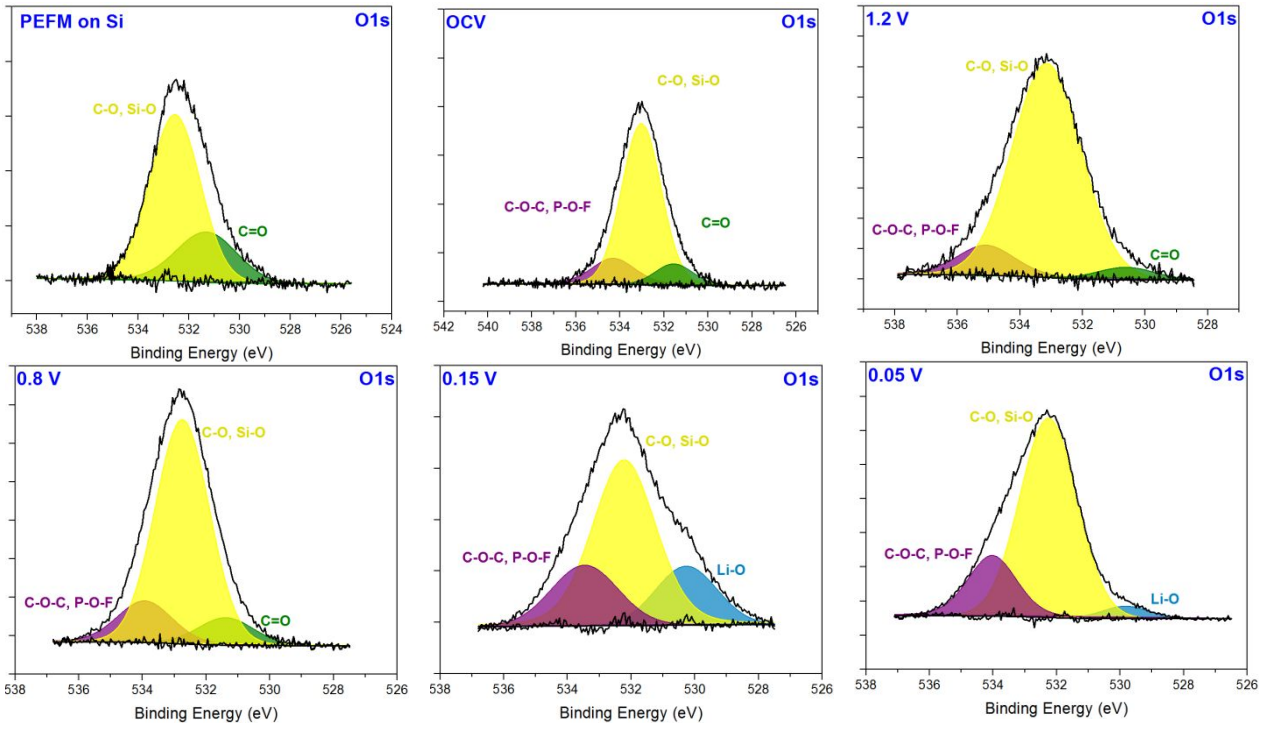

Figure 4. XPS results for O1s spectra

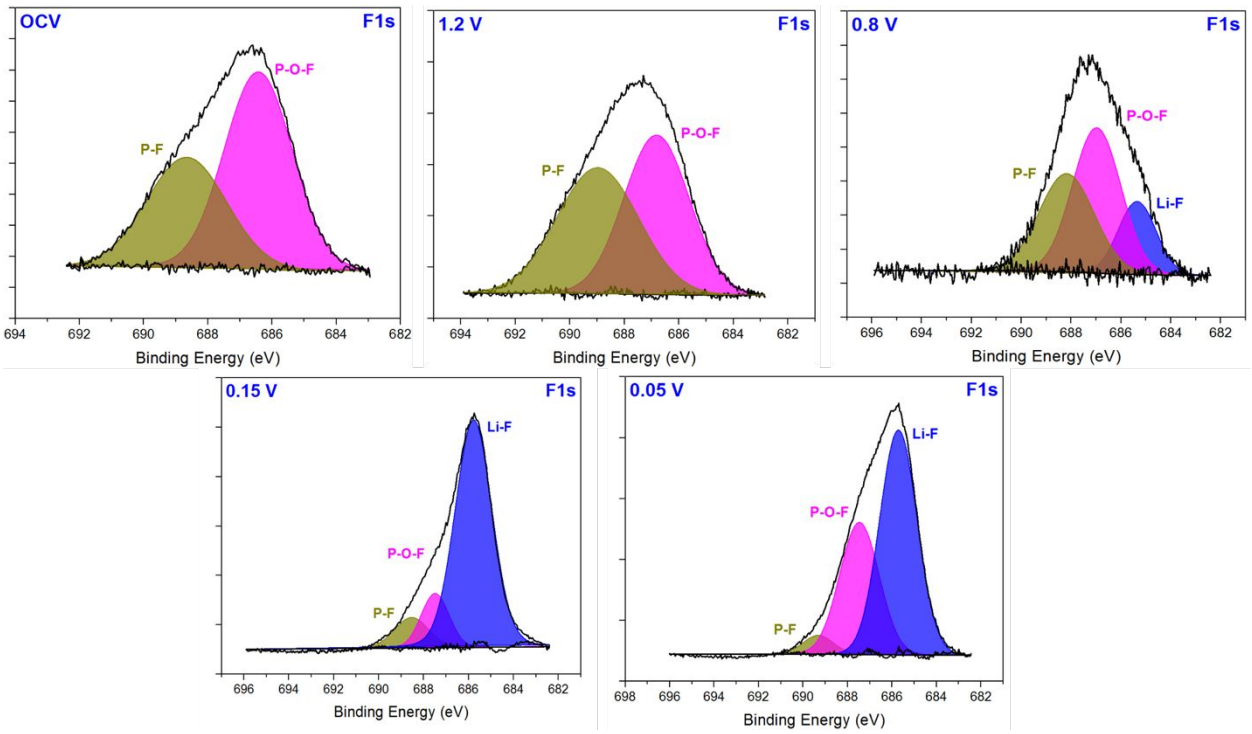

Figure 5. XPS results for F1s spectra

No Lithiation (1.5 and 1.2 V). Previous experiments have indicated trace impurities could be present within the deuterated solvents and as a precaution the 1.5 V (vs. Li/Li^+) potential is run at a higher C-rate to purify the electrolyte.(11) No change in the SLD of the electrolyte was observed between OCV and the 1.5 V potential, remaining at 5.46 indicating no significant impurities within the electrolyte; therefore, this parameter was kept constant for the remainder of the fits. No changes are evident in the film heterostructures at 1.5 V as indicated by NR refinements.

At 1.2 V the SLD increases from 1.59 to 2.58 in the PEFM layer from the incorporation of electrolyte accounting for upwards of 26% volume fraction which is also confirmed by a ~ 50 Å thickness increase from OCV and 1.5 V. The SLD of the reaction layer increased to 4.08 indicating higher SLD components from the electrolyte reacting in the reaction layer on the surface of the a-Si anode commensurate with a ~ 16 Å growth in thickness, Table 1. The XPS witness sample showed a decrease in the overall C content by approximately 10 at% (61 to 51 at%) as depicted in Figure S5 and the formation of a new spectra with a binding energy at 288.2 eV consistent with the formation of O-C=O (Figure 3). The O1s spectra showed an increase in the C-O, Si-O peak by approximately 10 at% from the OCV content of 76 at% with a subsequent decrease in C=O from 9.54 to 3.13 at% (Figure S6).

Initial SEI Formation (0.8 V). Refinements of the 0.8 V NR data indicates two distinct structures: the SEI layer on the surface of the anode and the PEFM on top of the SEI as depicted in Figure 2 by the purple SLD profile. The interface between the SEI and PEFM are distinct and well defined. The electrochemistry as a function of state of charge and current is depicted in Figure 6, highlighting the large current response resulting in the generation of 2 coulombs of charge at 0.8 V (Figure 6). The most likely explanation is binding of Li to the PEFM, which is designed to be cathodically doped in a reducing environment where Li will attach to the F group of the polymer.(7) This is in conjunction with an increase in thickness of the PEFM to ~ 200 Å, from 93 Å from the previous potential. The significant increase in SLD of the PEFM layer to 5.21 (from 2.58) suggests a large incorporation of solvent within the polymer layer. Interestingly, NR shows no increase in thickness for the SEI (from the previous potential). However, there is a significant increase in the SLD from 4.08 at 1.2 V to 5.52 indicative of a significant change in chemistry of the SEI layer on the surface of the Si due to the reduction of the d-EC at this potential or uptake of Li^+ into the bottom of the PEFM from the SEI layer. The close SLD value of the SEI layer at 5.5 is close to the SLD of the electrolyte at 5.46 indicates the layer of close chemical composition to the electrolyte. The ability to see the layer is a result of the presence of the polymer which has a SLD of 5.21.

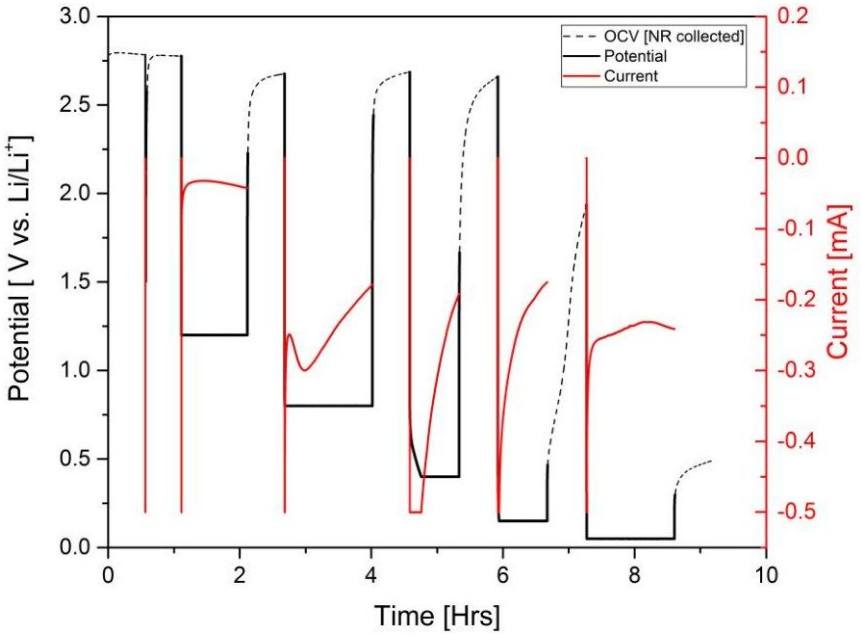

Figure 6. Electrochemical data for *in situ* neutron experiment with voltage profile highlighted in solid black and current profile highlighted in red. Neutron collection occurred after cell returned to equilibrium highlighted by dashed black line.

The overall XPS spectra indicates an increase in the C content around 67.1 at%, up from 51.6 at% at 1.2 V; in addition, a slight increase of ~6 at% of O content from the as-prepared, OCV, and 1.2 V witness samples which averaged around ~12.3 at% (Figure S5). While a decrease in the inorganic moieties, F and P, indicating the 0.8 V SEI layer was organic in nature as depicted in Figure 7 which compares the organic portions (C, O) with the inorganic components (F, P) overlaid with the SEI thickness and SLD. This is in conjunction with the high SLD value observed. Looking at the results for fits in Figure S6 for C1s spectra, C-C/C-H species increased to 75 at% while a significant decrease in the C-O peak was observed (31.0 at% to 17.5 at%) and is also confirmed in the O1s spectra. The O-C=O moieties stayed the same. The O1s indicated a slight increase in the C-O-C, C-O-F as well as the C=O. The F1s and P2p both indicate a decrease in the P-O-F species. A new species was observed with a binding energy of 685.40 eV assigned to the formation of LiF (Figure 5). The XPS indicates an organic layer rich in C and O; however, a significant portion of this layer must have been removed with the rinsing of the witness sample as the Si^0 (Figure S2) is still evident even though NR indicates a polymer layer ~20 nm thick beyond the maximum escape depth of the photoelectrons. The SLD of the PEFM layer is ~5.14, close to that of the electrolyte (5.46) which is in agreement with the XPS indicating a large amount of C, D, O, F incorporation into the layer all of which have high scattering cross sections.

Beginning of Lithiation (0.4 and 0.15 V). The lithiation of the a-Si layer begins at 0.4 V vs Li/Li^+ as indicated in the NR refinements with the increase in the Si layer thickness from 472.5 to 484.5 Å. This is coupled with the lowering of the SLD to 1.92 (Table 1) indicating the incorporation of Li as it has a low scattering cross section which lowers the average SLD. From formalism developed by Chevrier and Dahn(17) the extent of lithiation was estimated to be $Li_{0.05}Si$, a very small Li content within the Si. Li is also becoming incorporated in the SEI layer as a significant decrease in the SLD, from 5.52 to 4.57, was observed as well as a swelling of the layer by over 70 Å (compared to the 0.8 V thickness). There is evidence of a more intermixed layer forming between the polymer and SEI as observed in the SLD profile (Figure 2) in which the distinct polymer layer at 0.8 V is no longer evident at 0.4 V. The SLD profile indicates a diffuse interface

between the SEI and polymer layer. The large uptake of electrolyte results in a contrast match as the layers' SLD become close to that of the electrolyte. By 0.15 V the PEFM and SEI layers results in a gradient where the interface between the two layers is no longer distinguishable. Interestingly, the SLD of the PEFM layer has decreased from 5.19 to 4.62 similar to the SEI layer which settles to 3.91 (as compared to 4.47 at 0.4 V) as shown in Figure 7. As the potential is decreasing and more Li^+ is moving through the system it is most likely becoming incorporated in the PEFM as well as being consumed in the SEI leading to the small Li:Si ratio, $Li_{0.09}Si$, being observed. The Si layer has only slightly changed in both thickness and SLD further supporting low concentrations of Li^+ in the anode.

XPS supports a thick layer formation as indicated by the intensity of the Si2p peak which has significantly decreased due to the attenuation of the photoelectrons from the surface of the electrode. The overall C content decreases going from 0.8 to 0.15 V by as much as 46 at%, going from 67.1 at% at 0.8 V to 20.7 at% at 0.15 V (Figure S5). The Li content accounting for 41.6 at%, is likely representative of the top layers of the sample both in the PEFM and SEI layers as opposed to the Si itself due to the thickness, ~ 800 Å of the two layers determined by NR. A significant amount of the layer mush have been washed off due to the presence of Si2p spectrum (Figure S2). Charging was observed in the sample and found to be caused by the increased LiF species which is insulating in nature (as depicted by the grey peak in Figure 3). The LiF content increased from 17.7 at % to 76.7 at%. The high content of LiF implies extensive reduction of the $LiPF_6$ salt. This is further supported by the Li1s spectra which is entirely composed of LiF (56.15 eV). No significant changes in the P2p were observed. The C-C/C-H peak decreased significantly (27.2 at% total) while the C-O moieties increased from 17.5 to 40.2 at%. A new peak with a binding energy of 289.8 eV was observed and assigned to $-CO_3$ while no O-C=O was evident. Figure 4 shows the formation of a new species in the O1s spectra with a binding energy of 530.2 eV attributed to Li-O species.

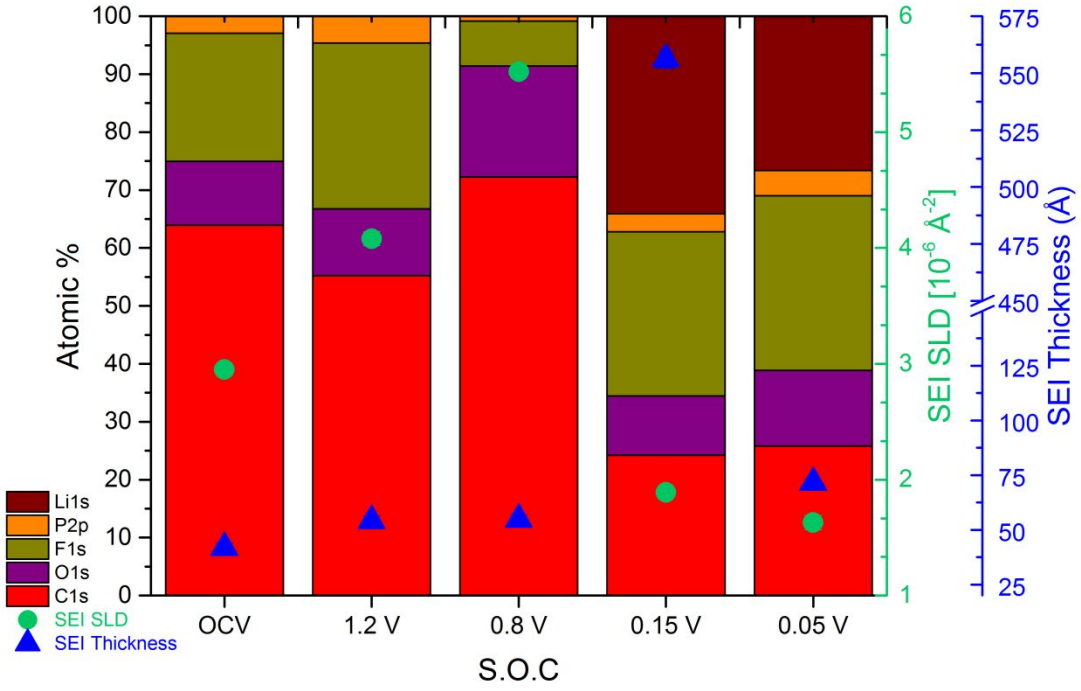

Figure 7. Atomic % of XPS witness samples at various states of charge overlaid with SEI SLD (green circle) and SEI thickness (blue triangle).

Lithiated (0.05 V). At 0.05 V the a-Si layer has been lithiated to $Li_{0.7}Si$ based on thickness. Due to the low Li:Si ratio the Li was most likely consumed in the both the SEI and PEFM layer which is further evidenced by a decrease in the SLD of the SEI (3.91 to 1.63) and that of the PEFM (3.09 from 4.62). The SEI and PEFM layer/s appear to swell significantly at 0.15 V; however, at 0.05 V a distinct 71.6 Å SEI layer forms on the surface of the lithiated a-Si with an SLD of 1.63 (Figure 2, Table 1). This would indicate a fairly Li rich SEI due to the significant decrease in SLD from the previous two voltage states. Lithiation is also indicated by an increase in the a-Si layer increasing to 747.9 Å and lowering of the SLD to 0.43 indicative of Li^+ incorporation. The PEFM layer is most likely trapping Li as the lithiated Si layer has not reached the theoretical limit of $Li_{3.75}Si$. The PEFM layer compresses to 121.3 Å, a decrease of ~ 126 Å from the previous potential, as is crosslinks or expels solvent. Components within the PEFM layer are being dissolved back into the electrolyte. The Si2p peak points to the lithiation of an oxide layer on the surface of the Si as a peak consistent with Si-O-F is identified. However, given the total thickness of the surface layers on the surface of the anode, ~193 Å, a significant portion of the layers are being rinsed away. The XPS confirms a Li_2O peak with a binding energy of 55.8 eV as well as a

significant amount of LiF. The insulating nature of both the LiF and Li-O resulted in significant charging evident in the C1s peak. The F1s and P2p peaks both show an increase in the P-O- species.

Discussion

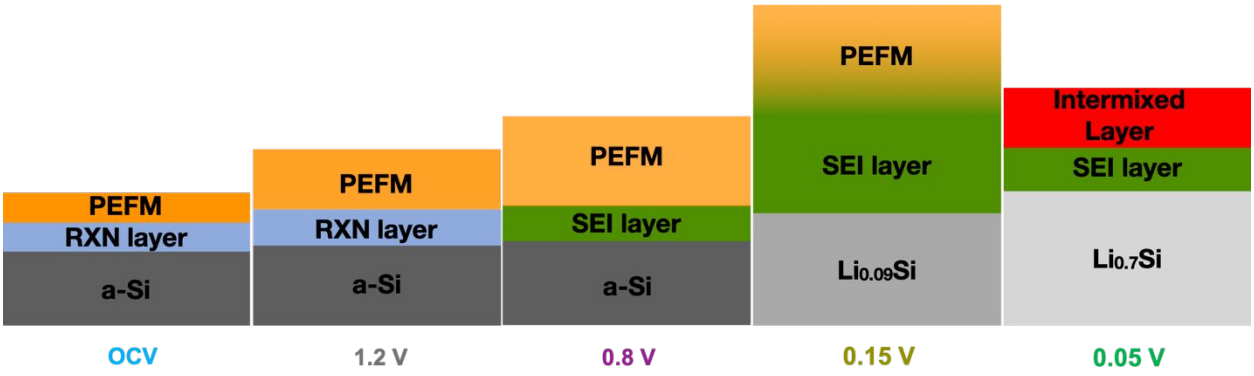

Figure 8. Summary of heterostructures from NR refinements at various states-of-charge

The effect of the polymer binder, PEFM, on the SEI composition and formation on a Si anode is explored in the presented data through the use of *in situ* NR and *ex situ* XPS. A schematic of the film heterostructures, as determined by the NR refinements, is depicted in Figure 8. From the NR it is evident the polymer layer is continuously changing with higher states of lithiation through interactions with the electrolyte. At OCV, Li is concentrated at the surface of the anode, underneath the PEFM, in the reaction layer and a similar thickness and SLD is evident when compared to previous NR experiments (Table 2).(10,11,13) As the cell is polarized to 1.2 V, the swelling of the PEFM layer is observed commensurate with an increase in SLD due to solvent uptake. There is a small increase in the SEI SLD due to D, C, O, F species (Figure 3), but not much change in the thickness of the SEI layer. At 0.8 V we observe a huge increase in the PEFM thickness and composition (increased SLD) which has to be due to solvent incorporation/swelling. We continue to see the SEI grow more organic due to solvent decomposition. This is further supported by the XPS results which shows a distinct Si spectrum of the witness sample (Figure S2), as the polymeric/organic moieties are more susceptible to the rinsing procedure and would be redissolved in the wash which explains the much thinner layer observed in XPS at 0.8 V.(18)

At 0.4 V a thinning in the PEFM layer occurs in addition to swelling of the SEI to 130 Å with a small drop in SEI SLD (5.5 to 4.5) due to more solvent and more Li within in the SEI layer. If it was just related to solvent the SLD would be higher, whereas if it were related to salt alone

the SLD would be much lower. The two layers (PEFM and SEI) are closely mixed and appear to be transferring solvent (C, O, F, D) from the PEFM to SEI resulting in a matrix between the two layers. The 0.15 V data shows a growth in the PEFM again through solvent and salt incorporation, but there is a larger swelling of the SEI layer to 556 Å corresponding with a decrease in the SLD which occurs because of solvent and salt concentration. The PEFM binder was designed to swell in electrolyte solutions, similar to PVDF, and shown to incorporate upwards of 50 wt% of solvent within its structure.(7,19) The significant electrolyte uptake within the PEFM inhibits the bulk electrolyte from contacting the Si surface. The most likely explanation for a matrix from the electrolyte/PEFM/SEI interfaces, observed at 0.4 and 0.15 V is the result of electrolyte decomposition within the polymer and SEI layer altering the electrolyte composition that is interacting with the Si. This was recently observed in another binder poly (1-pyrenemethyl methacrylate) (PPy). (20) The authors from this study determined the mechanism for passivation of the crystalline Si, in the presence of the PPy binder, was altered as a result of selective solvent uptake. This changed the distribution of the decomposition products resulting in ineffective passivation of the Si surface.(20)

At 0.05 V a condensation process is observed in the PEFM/SEI matrix resulting in a now well-defined SEI layer on the surface of the lithiated Si (Figure 2 bottom green SLD plot). The PEFM is 121 Å with an SLD of 3.1 indicating less organics within the layer, while the SEI goes from 556 to 71 Å and an SLD of 3.9 to 1.6. Again, a less organic but Li^+ rich SEI layer. Once the cell is polarized to 0.05 V there is enough of a driving force to push unreacted Li^+ in the layers into the anode causing a reordering of the SEI and PEFM. However, due to the elemental makeup the PEFM layer is no longer the same as the as prepared resulting in an intermixed layer of electrolyte decomposition products and PEFM (Figure 8). The contraction of the SEI is a result of the changing composition and density of the layer. Due to the two unknowns within Equation 2, the density and exact chemical composition of the SEI layer cannot be determined from NR alone.

In comparison with previous work done by the group looking at a-Si anode in the same electrolyte(11) and with addition of the electrolyte additive (FEC),(13) there are evident trends among the three cases (Table 2). The OCV reaction layer among all three experiments is similar in thickness and SLD, indicating similar reaction mechanism and chemical compositions. At 1.2 V, the PEFM and Si show a more organic SEI on the surface of the Si with similar chemical

compositions.(11) Interesting, in the case of the FEC the SLD remained fairly consistent throughout and is fairly Li^+ rich. However, both the Si and FEC become inorganic as the cell is further polarized [0.4 to 0.15 V], while the PEFM remains organic. Together this data indicates the FEC is driving the surface far more inorganic in nature, while the PEFM promotes organic like interfaces. After lithiation the SEI always becomes mostly inorganic, but the PEFM delays this transition. Unlike the two previous cases, it is evident there is a bilayer present on the surface of the lithiated Si with a total thickness of ~193 Å. A dense and compact layer on the surface of the anode that is Li^+ rich, and a more organic layer at the electrolyte interface similar to the suggested bilayer SEI structure.(21)

Table 2. A comparison of SEI thicknesses and SLDs from NR experiments of PEFM, a Si anode, and Si with FEC additive.

	PEFM		Si (11)		FEC (13)	
	SEI [Å]	SLD [10^{-6} Å^{-2}]	SEI [Å]	SLD [10^{-6} Å^{-2}]	SEI [Å]	SLD [10^{-6} Å^{-2}]
OCV	42	3.0	45	2.4	60	2.6
1.2	55	4.1	175	4.7	58[a]	2.6[a]
0.4	130	4.5	246	2.0	59	2.6
0.15	556	3.9	187[b]	2.9[b]	68	2.3
0.05	72	1.6				
ORGANIC → INORGANIC						
C, O, D					Li^+	

[a]Data collected at 0.9 V vs. Li/Li^+, [b]Data collected at 0.12 V vs. Li/Li^+

The data points to the PEFM acting as a membrane where solvent molecules selectively concentrate to the surface of the Si. The PEFM acts as a barrier to lithiation of the anode, then is gets polymerized/condensed where it appears organics are redissolved into the electrolyte. The swelling of the PEFM binder is similar to what is observed for PVDF.(3,22,23) Beyond the mechanical properties of the PVDF binder, the uptake of electrolyte within the binder system maybe determinantal to the performance of the Si cell. This hypothesis needs to be explored. If a

polymer system could be designed to drive the salt to the surface with selective ion transport it may yield a better SEI and a "stable" Si anode.

Conclusion

This study highlights the complicated role of the binder in SEI formation. The PEFM binder is a dynamic layer that hinders the lithiation of the anode until low potentials and concentrates organic solvent near the surface. There is a defined interface between the SEI and binder layer indicating the SEI still forms on the surface of the anode as opposed to the surface of the PEFM and a bilayer structure is evident at 0.05 V. This study focused on a model electrode representing a fully coated active particle. It would suggest that patchy coating of the binder would result in a different SEI formation and thickness; however, with the full coating of the binder a distinct two-layer SEI is observed on the surface of the lithiated anode. The membrane like behavior of the polymer indicates a binder that selectively brings salt to the surface, in addition to ion channels would perform better as opposed to uptake of solvent molecules.

Acknowledgments

This research at the Oak Ridge National Laboratory, managed by UT Battelle, LLC, for the U.S. Department of Energy (DOE) under contract DE-AC05-00OR22725 was sponsored by the Office of Energy Efficiency and Renewable Energy (EERE) Vehicle Technologies Office (VTO) (Deputy Director: David Howell) SEISTa subprogram (Program Manager: Brian Cunningham) (KLB and GMV) and the Office of Basic Energy Sciences FWP-ERKCSNX (JFB, MD). The neutron experiment at the Materials and Life Science Experimental Facility of the J-PARC (NY) was performed under a user program (Proposal No. 2017AU1602).

References

1. Beaulieu LY, Eberman KW, Turner RL, Dahn JR, Krause LJ. Colossal Reversible Volume Changes in Lithium Alloys. Electrochem Solid-State Lett. 2002;4(9):A137.
2. Obrovac MN, Krause LJ. Reversible Cycling of Crystalline Silicon Powder. J Electrochem Soc [Internet]. 2007;154(2):A103. Available from: http://jes.ecsdl.org/cgi/doi/10.1149/1.2402112

3. Magasinski A, Zdyrko B, Kovalenko I, Hertzberg B, Burtovyy R, Huebner CF, et al. Toward efficient binders for Li-ion battery Si-based anodes: Polyacrylic acid. ACS Appl Mater Interfaces. 2010;2(11):3004–10.
4. Liu W-R, Yang M-H, Wu H-C, Chiao SM, Wu N-L. Enhanced Cycle Life of Si Anode for Li-Ion Batteries by Using Modified Elastomeric Binder. Electrochem Solid-State Lett [Internet]. 2005;8(2):A100. Available from: http://esl.ecsdl.org/cgi/doi/10.1149/1.1847685
5. Li J, Lewis RB, Dahn JR. Sodium Carboxymethyl Cellulose. Electrochem Solid-State Lett [Internet]. 2007;10(2):A17. Available from: http://esl.ecsdl.org/cgi/doi/10.1149/1.2398725
6. Li J, Le D-B, Ferguson PP, Dahn JR. Lithium polyacrylate as a binder for tin–cobalt–carbon negative electrodes in lithium-ion batteries. Electrochim Acta [Internet]. 2010 Mar;55(8):2991–5. Available from: https://linkinghub.elsevier.com/retrieve/pii/S0013468610000599
7. Wu M, Xiao X, Vukmirovic N, Xun S, Das PK, Song X, et al. Toward an Ideal Polymer Binder Design for High-Capacity Battery Anodes. J Am Chem Soc [Internet]. 2013 Aug 14;135(32):12048–56. Available from: http://pubs.acs.org/doi/10.1021/ja4054465
8. Jeschull F, Maibach J, Félix R, Wohlfahrt-Mehrens M, Edström K, Memm M, et al. Solid Electrolyte Interphase (SEI) of Water-Processed Graphite Electrodes Examined in a 65 mAh Full Cell Configuration. ACS Appl Energy Mater [Internet]. 2018 Sep 18;acsaem.8b00608. Available from: http://pubs.acs.org/doi/10.1021/acsaem.8b00608
9. Nguyen CC, Yoon T, Seo DM, Guduru P, Lucht BL. Systematic Investigation of Binders for Silicon Anodes: Interactions of Binder with Silicon Particles and Electrolytes and Effects of Binders on Solid Electrolyte Interphase Formation. ACS Appl Mater Interfaces [Internet]. 2016 May 18;8(19):12211–20. Available from: http://pubs.acs.org/doi/10.1021/acsami.6b03357
10. Veith GM, Baggetto L, Sacci RL, Unocic RR, Tenhaeff WE, Browning JF. Direct measurement of the chemical reactivity of silicon electrodes with LiPF6-based battery electrolytes. Chem Commun [Internet]. 2014;50(23):3081. Available from: http://xlink.rsc.org/?DOI=c3cc49269a
11. Veith GM, Doucet M, Baldwin JK, Sacci RL, Fears TM, Wang Y, et al. Direct Determination of Solid-Electrolyte Interphase Thickness and Composition as a Function of State of Charge on a Silicon Anode. J Phys Chem C [Internet]. 2015 Sep

3;119(35):20339–49. Available from: http://pubs.acs.org/doi/10.1021/acs.jpcc.5b06817

12. Cao C, Steinrück HG, Shyam B, Toney MF. The Atomic Scale Electrochemical Lithiation and Delithiation Process of Silicon. Adv Mater Interfaces. 2017;4(22):1–7.
13. Veith GM, Doucet M, Sacci RL, Vacaliuc B, Baldwin JK, Browning JF. Determination of the Solid Electrolyte Interphase Structure Grown on a Silicon Electrode Using a Fluoroethylene Carbonate Additive. Sci Rep [Internet]. 2017 Dec 24;7(1):6326. Available from: http://dx.doi.org/10.1038/s41598-017-06555-8
14. Yamada NL, Torikai N, Mitamura K, Sagehashi H, Sato S, Seto H, et al. Design and performance of horizontal-type neutron reflectometer SOFIA at J-PARC/MLF. Eur Phys J Plus [Internet]. 2011 Nov 11;126(11):108. Available from: http://www.springerlink.com/index/10.1140/epjp/i2011-11108-7
15. Mitamura K, Yamada NL, Sagehashi H, Torikai N, Arita H, Terada M, et al. Novel neutron reflectometer SOFIA at J-PARC/MLF for in-situ soft-interface characterization. Polym J [Internet]. 2013 Jan 5;45(1):100–8. Available from: http://dx.doi.org/10.1038/pj.2012.156
16. Nelson A. Co-refinement of multiple-contrast neutron/X-ray reflectivity data using MOTOFIT. J Appl Crystallogr [Internet]. 2006 Apr;39(2):273–6. Available from: https://doi.org/10.1107/S0021889806005073
17. Chevrier VL, Dahn JR. First Principles Model of Amorphous Silicon Lithiation. J Electrochem Soc [Internet]. 2009;156(6):A454. Available from: http://jes.ecsdl.org/cgi/doi/10.1149/1.3111037
18. Fears TM, Doucet M, Browning JF, Baldwin JKS, Winiarz JG, Kaiser H, et al. Evaluating the solid electrolyte interphase formed on silicon electrodes: A comparison of: Ex situ X-ray photoelectron spectroscopy and in situ neutron reflectometry. Phys Chem Chem Phys. 2016;18(20):13927–40.
19. Wu M, Song X, Liu X, Battaglia V, Yang W, Liu G. Manipulating the polarity of conductive polymer binders for Si-based anodes in lithium-ion batteries. J Mater Chem A [Internet]. 2015;3(7):3651–8. Available from: http://xlink.rsc.org/?DOI=C4TA06594H
20. Haregewoin AM, Terborg L, Zhang L, Jurng S, Lucht BL, Guo J, et al. The electrochemical behavior of poly 1-pyrenemethyl methacrylate binder and its effect on the interfacial chemistry of a silicon electrode. J Power Sources [Internet]. 2018 Feb;376:152–

60. Available from: https://linkinghub.elsevier.com/retrieve/pii/S0378775317315276

21. Peled E. Advanced Model for Solid Electrolyte Interphase Electrodes in Liquid and Polymer Electrolytes. J Electrochem Soc [Internet]. 1997;144(8):L208. Available from: http://jes.ecsdl.org/cgi/doi/10.1149/1.1837858

22. Chen Z, Christensen L, Dahn JR. Comparison of PVDF and PVDF-TFE-P as Binders for Electrode Materials Showing Large Volume Changes in Lithium-Ion Batteries. J Electrochem Soc [Internet]. 2003;150(8):A1073. Available from: http://jes.ecsdl.org/cgi/doi/10.1149/1.1586922

23. Komaba S, Shimomura K, Yabuuchi N, Ozeki T, Yui H, Konno K. Study on Polymer Binders for High-Capacity SiO Negative Electrode of Li-Ion Batteries. J Phys Chem C [Internet]. 2011 Jul 14;115(27):13487–95. Available from: https://pubs.acs.org/doi/10.1021/jp201691g